Semiconductor Physics, Quantum Electronics & Optoelectronics, 2025. V. 28, No 1. P. 059-069.

Optoelectronics and optoelectronic devices

Comparison of optical and photovoltaic characteristics of solar cells based on heterojunctions of organic nanocomposite films on Si and GaAs

S.V. Mamykin[1,2*], T.S. Lunko[1], I.B. Mamontova[1], O.S. Kondratenko[1], T.R. Barlas[1], N.V. Kotova[1], T.V. Semikina[1], I.M. Dmitruk[2], N.I. Berezovska[2], Ye.S. Hrabovskyi[2], V.R. Romanyuk[1]

[1]*V. Lashkaryov Institute of Semiconductor Physics, NAS of Ukraine, 41 Nauky Avenue, 03028 Kyiv, Ukraine*
[2]*Taras Shevchenko National University of Kyiv, 4 Hlushkova Avenue, 03022 Kyiv, Ukraine*
[*]*Corresponding author e-mail: mamykin@isp.kiev.ua*

Abstract. Comparison between solar cell heterostructures based on poly(3,4-ethylenedioxythiophene)-poly(styrene-sulfonate) (PEDOT:PSS) organic complex thin film and semiconductors (Si, GaAs) with flat and microrelief interfaces have been performed. PEDOT:PSS film thicknesses and optical parameters were ascertained using spectroscopic ellipsometry, while electrical dc-conductivity was determined using the four-point probe method. A method of increasing the conductivity of PEDOT:PSS films by forming a multilayer film with a decreased content of PSS component is proposed. Plasmon-active metal nanoparticles (Au, Ag) have been grown on the active interface region to increase photoconversion efficiency. They reduce the structure series resistance and increase the *I–V* characteristic fill factor as well as the incident light absorption. The post-processing treatment method of fabricated structures to obtain a tunnel-thin intermediate layer of SiO_2 of optimal thickness has been proposed. The photoelectric properties of the fabricated solar cells have shown that GaAs-based structures have more stable long-term characteristics and higher open-circuit voltage than Si-based ones.

Keywords: heterojunction, solar cells, microrelief, PEDOT:PSS, metal nanoparticles, post-treatment.

https://doi.org/10.15407/spqeo28.01.059
PACS 78.67.Bf, 81.07.Pr, 84.60.Jt

Manuscript received 13.11.24; revised version received 14.01.25; accepted for publication 12.03.25; published online 26.03.25.

1. Introduction

Recently, solar cells (SCs) based on organic materials have been actively developed due to the simple fabrication technology that can reduce the cost of converting solar energy into electrical energy. Today, one of the most popular organic semiconductors is the poly(3,4-ethylenedioxythiophene)-poly(styrene-sulfonate) (PEDOT:PSS) composite. PEDOT is a leading *p*-type organic conductive polymer that is electrochemically stable and optically transparent. The PEDOT:PSS composite is widely used in organic electronics, including the photosensitive heterostructures of the organic/inorganic semiconductor type. These structures, with promising characteristics, are easy to fabricate using the vacuum-free, low-temperature technology [1]. Recently, PEDOT:PSS/Si hybrid silicon-organic SCs with high solar energy conversion efficiency (14% and more) were obtained in many groups [2–4].

The role of PEDOT:PSS in these photovoltaic structures is multifaceted: a conducting and collecting frontal electrode, an antireflection coating, and a charge-selective layer that reflects electrons and extracts holes, thereby significantly reducing recombination [1]. PEDOT:PSS films, like other transparent conductive films, have good transparency within the spectral range of silicon photosensitivity. The conductivity of pure PEDOT:PSS films is low, equal to 1 S/cm, but it can be increased using physical and chemical approaches [5].

Among the large number of works aimed at ensuring high electrophysical parameters of PEDOT:PSS films, which must meet modern high standards for SC, we single out the following: achieving high electrical conductivity of PEDOT:PSS films, improving existing ones and searching for new methods of post-growth treatment of these films and their interface with inorganic semiconductors.

Since PEDOT:PSS has a high work function (~5.0 eV [6]), its contact with noble metals (Ag, Au) should be Ohmic. This opens up the possibility of improving the conductivity of PEDOT:PSS films by adding nanoparticles (NPs) of the mentioned metals. Moreover, it is possible to use the effects of the near-field enhancement of the electromagnetic wave by metal NPs, which directs the scattered light into the substrate and leads to an increase in absorption and a reduction of reflection losses [7–9]. Additional microtexturing of the semiconductor surface is also used to reduce reflection losses in solar cells, and greatly contributes to increasing their efficiency [10, 11].

The heterojunction interface in a photovoltaic converter has a critical effect on its efficiency. To reduce the recombination of photogenerated carriers, it is important to achieve a low density of surface states. To ensure this, it is important to create a stable tunnel-thin transparent (~1.2...1.5 nm) layer of SiO_2. The morphology of the thin polymerized PEDOT:PSS organic film is such that after evaporation of the solvent, it has a granular structure and contains a large number of nanopores and nanocavities. When the Si surface is exposed to the air, a native oxide will grow easily reaching a thickness equal to 3.1 nm [12]. It is possible to improve the contact characteristics at the PEDOT:PSS/Si interface (current transfer) and reduce the access of air to the open areas of the silicon surface by improving the wettability of the Si surface for PEDOT:PSS and reducing the porosity of polymer film.

In this paper, we present some approaches to increase the efficiency of organic/inorganic SC heterostructures based on PEDOT:PSS/Si(GaAs), namely semiconductor surface texturing, deposition of the noble metal (Ag, Au) nanoparticles, and post-growth treatment of fabricated structures. Additionally, the stability of the photoelectrical characteristics of SCs based on the PEDOT:PSS/GaAs heterojunction was studied.

2. Experimental details

2.1. Technologies of semiconductor interface modifications

The influence of some factors on the photoelectric properties of organic-inorganic heterojunction nanocomposite solar cells was studied in PEDOT:PSS/Si and PEDOT:PSS/GaAs heterostructures with flat and textured interfaces. Polished phosphorus-doped *n*-type silicon wafers with a resistivity of 0.5...2.4 Ohm·cm were used as a substrate to form structures with a flat or textured interface.

Nanotextured silicon surfaces (porous “black” silicon) were formed on *n*-Si (100) substrates by metal-assisted chemical etching (MACE) [13] initiated by silver nanoclusters. A two-stage processing of the substrates was used. At the first stage, silver nanoclusters of 10...20 nm in size were grown by an electroless chemical photoinduced deposition from an aqueous solution of $AgNO_3$:HF:H_2O (HF:H_2O at a component ratio of 1:4 and an $AgNO_3$ concentration of 8 mM) for 20 s. The second stage of chemical treatment was the metal nanoparticles catalyzed pore etching in silicon wafers with a solution of H_2O_2:HF:H_2O (1:2:10) for 2 min at room temperature [14]. In this way, the pattern of surface coating with metal nanoparticles directly determines the places on the semiconductor substrate where etching of pores occurs.

Microtextured quasigrating-type surfaces were formed on *n*-Si (110) wafers by wet anisotropic chemical etching in a 20...30% aqueous solution of KOH at 60...75 °C for 35...50 min.

A quasigrating-type microrelief was formed as well on the (100) surface of the *n*-GaAs wafer with a dopant concentration of 10^{17} cm^{-3} by anisotropic wet chemical etching in a mixture of H_2SO_4:HF:H_2O_2 at 22...24 °C for 1...2 min [15, 16].

Gold nanoparticles were deposited on the GaAs surface (flat or quasigrating type) by photostimulated electroless chemical deposition from an aqueous solution of $AuCl_3$ salt (Au^{3+} ion concentration – 0.05 mg/cm^3, deposition time – 1.5 min) [17].

2.2. Fabrication of PEDOT:PSS/Si(GaAs) heterojunctions and solar cell heterostructures

Organic-inorganic heterojunction was formed by depositing thin organic *p*-type semiconductor film from an aqueous emulsion of PEDOT:PSS (Sigma-Aldrich, 2 wt.%) on the semiconductor surface. Dimethyl sulfoxide (DMSO) (5 wt.%) additive was used to increase the polymer conductivity by secondary doping [3]. To ensure the wettability of the hydrophobic surface of Si, the sodium dodecyl sulfate (SDS) [18] or Triton X-100 [19] surfactants were added in an amount of 2 wt.%. Before PEDOT:PSS deposition, the surface oxide was removed from all Si substrates by the 10% HF solution and using the 10% HCl for GaAs substrates. The single-layer film of PEDOT:PSS was deposited using a spin coating method at rotation frequency $\omega = 3000$ rpm. The obtained films were annealed using a hotplate at 140...150 °C in an air atmosphere for 30 min [20].

2.3. Sample characterization techniques

Surface morphology of the textured substrates was studied using AURA-100 (Saeron Technology) scanning electron microscope (SEM).

Optical parameters and thickness of thin films and resulting structures were investigated using SE-2000 (Semilab Ltd.) spectroscopic ellipsometer within the spectral range 250…2100 nm in the external reflectance collecting measurements at three angles of light incidence (65°, 70° and 75°). The width of the focused beam was equal to 0.4 mm on the sample surface.

Sheet resistance R_{SQ} was measured on the film surface using the collinear four-point probe method exploiting a CHI660E workstation (CH Instruments) with the probes positioned in line with a 1 mm distance. The electrical dc-conductivity of the films (σ) was calculated using the equation $\sigma = 1/(R_{SQ}\, d)$, where d is the film thickness [21].

The dark (direct and reverse) and light current-voltage (*I–V*) characteristics were measured under AM0 simulated illumination with a radiation power of $P = 136$ mW/cm^2.

3. Results and discussions

Typical SEM images of the flat, porous and quasigrating Si surfaces with Ag NPs covered by a thin layer of PEDOT:PSS are presented in Fig. 1. One can see that electroless metal deposition leads to formation of 10...50 nm noble metal nanoparticles on the semiconductor surface. Applying the MACE method, a porous layer of Si was formed with pores diameter equal to 10...50 nm (Fig. 1b) and an average depth equal to 300...380 nm. The period of quasigrating-type relief is 3...5 μm, while the average depth is 200...400 nm (Fig. 1c).

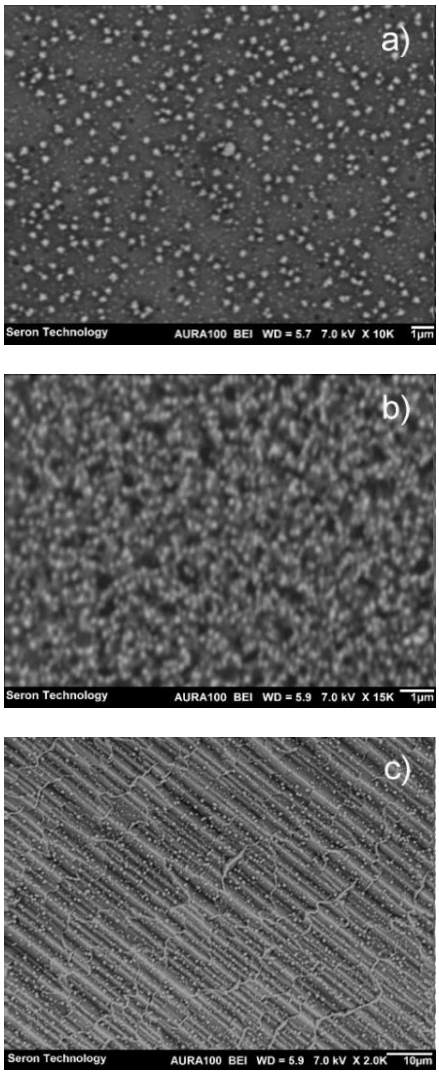

Fig. 1. SEM images of the Si surface with PEDOT:PSS layer and Ag NPs for flat (*a*), porous Si (*b*), and quasigrating-type (*c*) interfaces. Ag NPs were electroless deposited on the flat and quasigrating interfaces (*a, c*) after relief formations, while for the porous Si (*b*) they remained after MACE etching.

3.1. Optical and electrical properties of PEDOT:PSS thin films

Generally, when forming antireflection coating the film thickness d should satisfy the relation $d = \lambda/(4n)$, where n is the refractive index of the film. For the wavelength of the solar spectrum maximum intensity (550 nm) at $n \sim 1.5$, the effective film thickness d should be equal to 90 nm.

It is known that the polymerized PEDOT:PSS film showed a paracrystalline structure with highly conductive PEDOT nanocrystals uniformly distributed in the non-conductive PSS matrices [5, 22]. To create or improve the conditions for tunneling of charge carriers between PEDOT grains close contact and percolation between grains are critical. The PSS component from the thin polymerized PEDOT:PSS film can be partially dissolved and removed by washing with an organic solvent [23–27]. To reduce the number of cavities in the polymer film which are formed after its annealing, and to increase the content of the conductive PEDOT component, the films were formed using multiple deposition of PEDOT:PSS. Namely, after deposition and annealing of each layer, it was washed with ethyl alcohol followed by a study of the thickness and conductivity of such a multilayer film.

Considering that PEDOT:PSS films belong to the class of transparent conductive coatings the spectral behavior of dielectric permittivity $\varepsilon(E)$ of these films within the wide spectral range can be expressed by the sum of the classical Lorentz and Drude oscillators:

$$\varepsilon(E) = \varepsilon_\infty + \frac{A}{E^2 - E_L^2 + iE\cdot\Gamma_L} - \frac{E_p^2}{E^2 - iE\cdot\Gamma_p}. \qquad (1)$$

Here, E is the energy of incident light quanta ($E = 1.24/\lambda$), ε_∞ considers a contribution of high-frequency oscillators, E_L and E_p are the energies of the Lorentz (bound) and plasma (free carriers) oscillations, Γ_L and Γ_p are the damping parameters of these oscillations, and A is the Lorentz oscillator strength. Dielectric permittivity is expressed as $\varepsilon(E) = (n(E) + ik(E))^2$, where n and k are the refractive index and absorption coefficient, respectively.

The Lorentz component (second term in Eq. (1)) describes the optical properties of PEDOT:PSS within the UV-visible range, where polymer film possesses low absorbance and considerable transparency. The Drude component (third term in Eq. (1)) describes the interaction of light with free carriers in PEDOT:PSS. These terms separately and their sum are Kramers–Kronig consistent. This approach allows, in particular, avoiding the effect of inhomogeneity and other imperfections of the film structure on the result of determining optical parameters.

The film conductivity σ can be derived from optical measurements using the energy of plasma (free carriers) oscillations E_p, and the plasma oscillation damping parameter E_Γ, determined from optical modeling. In particular, the conductivity is [28]:

Table 1. Parameters of the optical model, thickness and conductivity of PEDOT:PSS multilayer films on Si, derived from spectroscopic ellipsometry and 4-point probe measurements.

Sample structure		1-layer as-prepared	1-layer washed	2-layer washed	3-layer washed	4-layer washed	5-layer washed	6-layer washed
Fit quality parameter, R^2 [28]		0.999	0.998	0.998	0.991	0.985	0.981	0.979
Rough overlayer thickness, nm		16.2	7.5	10.2	23.1	26	32	26.8
Film thickness, d, nm		83.4	41.7	82.7	131.4	186	235.3	288.9
Lorentz component	ε_∞	1.88	2.002	1.937	1.647	1.604	1.577	1.276
	A	0.408	0.435	0.385	0.532	0.492	0.468	0.756
	E_L, eV	6.355	6.979	5.929	6.251	6.526	6.681	7.735
	Γ_L, eV	0.700	1.202	0.522	0.506	0.522	0.690	0.782
Drude component	E_p, eV	0.398	0.022	0.268	0.906	1.003	0.972	0.928
	Γ_p, eV	2.06	4.798	3.708	2.612	1.374	1.086	0.846
Film conductivity from SE measurements, S/cm		9.4	0.01	2.8	42.3	98.5	117.1	137.0
Film dc-conductivity σ from four-point probe measurements, S/cm		106.5	47.4	108.3	168.9	235.9	149.1	193.5

$$\sigma = \frac{\varepsilon_0 E_p^2}{E_\Gamma \eta}, \qquad (2)$$

where ε_0 is the free-space permittivity, $\hbar$ is the reduced Planck constant.

A comparison of experimental ellipsometric data with calculations has shown that the optical behavior of the multilayer film is well described by the model of a two-layer film. The lower film is continuous and homogeneous, and the surface roughness (with the size of inhomogeneities much smaller than the wavelength of the incident radiation) can be modeled as a composite of two components – air and the material of the lower continuous layer, using the Bruggemann approximation.

The parameters of dielectric function approximation (Eq. (1)), thickness and conductivity of PEDOT multilayer films on Si substrate are presented in Table 1. The absolute value of the thickness of the surface rough layer is 10...15% of the film total thickness. It contains ~ 60% of the solid component and ~ 40% of the voids.

After washing the single-layer annealed film with ethanol, we have observed a significant reduction in the film thickness, approximately by half, as determined using spectroscopic ellipsometric measurements. At the same time, there was a substantial decrease in the film conductivity, which was confirmed by electrical measurements using the 4-point probe method. For 3-layer film with a step-by-step washing process, the total film thickness approaches that of an unwashed single layer while for the electrical conductivity of such a film, a 2-3 times increase is observed. Thus, it is possible to obtain an acceptable conductivity of the film with a small thickness, close to the optimum for an antireflection coating.

Spectral dependences of the optical parameters of PEDOT multilayer films of various thicknesses on Si substrate, presented in Fig. 2, show a gradual change in the properties from the dielectric to the conductive film with an increase in the number of layers and total film thickness. One can see that for the films with a small thickness (1-2 layers) the refractive index $n(\lambda)$ is almost constant within a wide spectral range. The extinction coefficient $k(\lambda)$ for these films within this range is close to 0, which may indicate poor film conductivity due to the absence of percolation between PEDOT globules and an essential fraction of voids in the films after solvent evaporation during annealing.

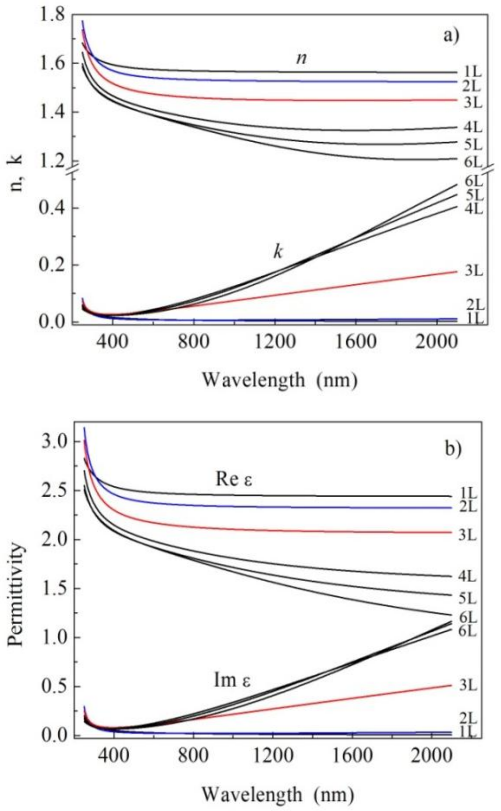

Fig. 2. Spectral dependences of the components of the complex refractive index $N = n + ik$ (*a*) and permittivity $\varepsilon = \varepsilon' + i\varepsilon'' = (n + ik)^2$ (*b*) of PEDOT:PSS multilayer (1L...6L) films of various thicknesses on Si substrates.

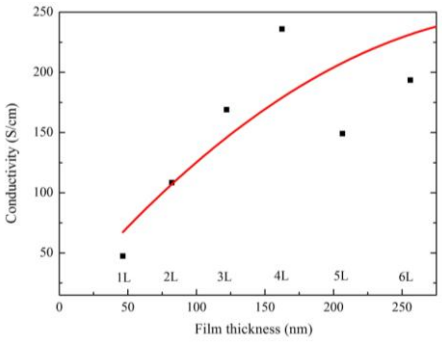

Fig. 3. Thickness dependence of the dc-conductivity (measured by the 4-point probe method) of a multilayer (1L...6L) PEDOT:PSS films.

With increasing the number of layers, better electrical contact between the PEDOT globules is obtained. The absorption coefficient k is increased gradually starting from a 3-layer film, especially within the near-IR (Drude) range. These changes also correlate with the data of conductivity measurements by the 4-point probe method presented in Fig. 3. The specific dc-conductivity of the films increases with increasing the number of deposited layers approaching saturation ($\sigma \sim 230$ S/cm) at thicknesses of $\approx$ 300 nm. This behavior can be probably attributed to the removal of PSS content during the washing, which subsequently allows the filling of the pores formed within the film with PEDOT conductive particles during the deposition of the next layer. As a result, this phenomenon enhances the contact between globules and leads to an overall increase in conductivity.

Another important effect, which should be considered is that PEDOT:PSS films have a globular structure with an average diameter of globules (D) of 60...70 nm [22, 29]. After subsequent deposition of the PEDOT:PSS layer followed by washing, a discrete increase in the total film thickness by approximately one monolayer of globules, approximately by $(2/3)^{1/2}D$, is observed (Table 1).

a. Photoelectric characteristics of SCs based on PEDOT:PSS/*n*-Si (*n*-GaAs) heterojunctions

Solar cell structures were fabricated basing on the obtained heterojunctions. Upper silver contacts in the form of a grid of 6×7 mm in size and 30...50 nm thick were deposited by thermal evaporation using a mask in a vacuum chamber. Ohmic back contacts were made by soldering indium onto a preliminarily cleaned Si surface with the 10% HF solution (Fig. 4).

I–V characteristics reflect all the processes occurring in solar cells and, in general, after correction for real devices with series and shunt resistance it can be described by a formula derived from the Shockley diode equation [30]:

$$I(U) = I_{ph} - I_0\left(\exp\left(\frac{q(U - IR_s)}{nkT}\right) - 1\right) - \frac{U + IR_s}{R_{sh}}, \qquad (3)$$

where I is the total current, I_{ph} is the photocurrent, I_0 is the saturation current, U is the voltage, R_s and R_{sh} are the series and shunt resistances of the structure, respectively,

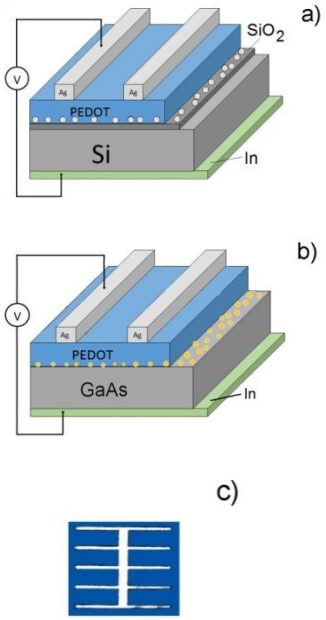

Fig. 4. Schematic representations of the SC structure design with the flat interface and Ag NPs on Si (a) and Au NPs on GaAs (b) substrates and the frontal image of the SC with the silver current-collecting grid of 6×7 mm (c).

n is the diode ideality factor, T is the temperature, k is the Boltzmann constant, and q is the electron charge. The efficiency of a solar cell can be determined using the following equation:

$$\eta = \frac{P_m}{P} = \frac{f I_{sc} U_{oc}}{P}, \qquad (4)$$

where P_m is the maximum power generated by the solar cell, P is the power of incident radiation on the solar cell, f is the fill factor of the *I–V* characteristic, I_{sc} is the short-circuit current and U_{oc} is the open-circuit voltage.

The dark and light *I–V* characteristics of the fabricated SC heterostructures measured under simulated illumination with a radiation power of P = 136 mW/cm^2 are shown in Figs. 5 and 6.

The parameters of solar cells (efficiency η, open-circuit voltage U_{oc}, short-circuit current I_{sc}, fill factor f, shunt R_{sh} and series R_s resistance) calculated based on the measured *I–V* characteristics are presented in Table 2.

The dark *I–V* characteristics of these structures are characterized by a large nonideality factor n (n = 2…6), which indicates a large contribution of the generation-recombination component [18] and a large effect of surface states at the PEDOT/Si interface.

In the case of textured interfaces, the effect of surface states is enhanced additionally by increasing the interface area, especially for a porous surface. The presence of Ag NPs at the PEDOT/Si interface also increases the recombination efficiency and, accordingly, the nonideality factor n. Therefore, light *I–V* characteristics of structures based on porous Si with Ag NPs show the worst results (the efficiency did not exceed 0.9...2.6%) even though a complete capture of incident

Table 2. Parameters of light *I–V* characteristics of SC heterostructures based on PEDOT:PSS/Si(GaAs).

Substrate	U_{oc}, mV	I_{sc}, mA/cm^2	*f*, %	R_s, Ohm	R_{sh}, Ohm	η, %
SDS surfactant						
Flat Si	561	35.8	30.3	16.4	30.1	4.5
Porous Si with Ag NPs	361	21.1	47.0	8.6	290.7	2.6
Quasigrating Si	461	39.4	32.9	6.2	17.2	4.4
Flat Si with post-treatment in 10% HF	500	42.4	47.3	3.7	75.3	7.3
Triton X-100 surfactant						
Flat Si with post-treatment in 10% HF	498	40.0	34.7	10.2	68.0	5.0
Flat Si with Ag NPs	486	33.7	50.6	4.5	274.1	6.1
Flat GaAs with Au NPs	566	22.4	57.5	3.7	210.1	5.4
Quasigrating GaAs with Au NPs	671	23.9	56.0	7.4	429.0	6.6

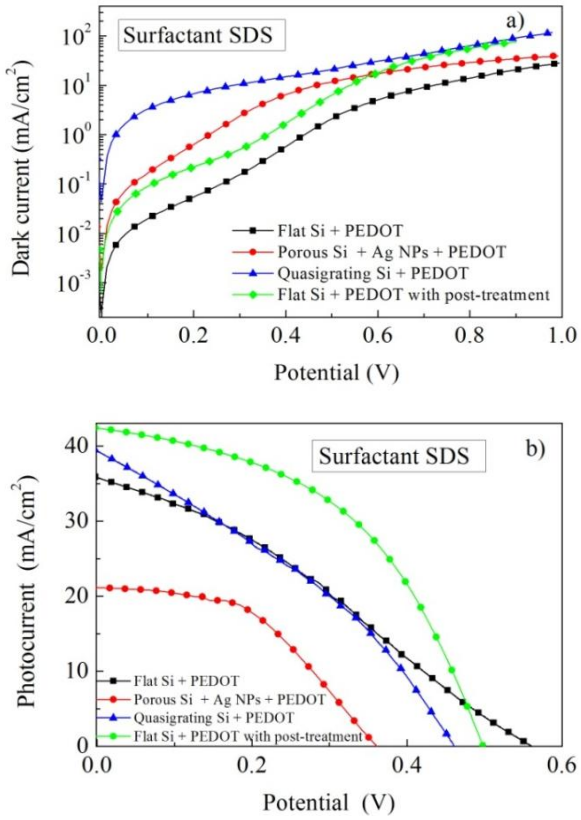

Fig. 5. Direct dark (*a*) and light (*b*) *I–V* characteristics of SC structures based on PEDOT:PSS/Si heterojunctions.

light occurs due to the enhanced electric field near Ag NPs and multiple scattering on the microrelief (Fig. 5).

Much better results are obtained for the structures, where Ag NPs are separated from the interface and deposited on the PEDOT layer. With the embedding of nanoparticles, the efficiency of the structure increases from 5% to 6.1%, primarily due to an increase in the filling factor *f* of the *I–V* characteristic from 34.7% to 50.6% (Fig. 5). This is because Ag NPs form an Ohmic contact with PEDOT, thereby improving the carrier collection by the front contact and decreasing the heterostructure series resistance R_s [31].

The microrelief of the quasigrating type expectedly increases the incident light capture. Thereafter the I_{sc} photocurrent increases from 35.8 to 39.4 mA/cm^2. Nevertheless, the efficiency remains almost unchanged – 4.4% due to a decrease in the open circuit voltage U_{oc} from 561 to 461 mV, which is typical for structures with a microrelief [1] (Fig. 5).

3.3. Stability of characteristics of SCs based on heterojunction with PEDOT:PSS

The efficient operation of a heterojunction solar cell depends on the properties of the interface between Si and PEDOT:PSS. The SiO_2 intermediate layer serves as a passivation coating for dangling Si bonds on the silicon surface. Simultaneously, it smoothes out surface irregularities and reduces the number of substrate defects, consequently lowering surface recombination [32]. It is known that the SiO_x layer changes the polarity of the Si surface from a negative dipole to a positive dipole [12].

The energy band of Si bends upwards. It leads to the alignment of the bonds between Si and PEDOT:PSS, which causes the separation of carriers and an increase in efficiency. However, a too thick layer of SiO_x prevents charge transfer, thereby reducing the open-circuit voltage and the fill factor [33]. For non-vacuum technology for obtaining organic SCs, the thickness of the SiO_2 layer can uncontrollably reach the thickness of native oxide on silicon. A gradual increase in the thickness of the oxide at the heterojunction boundary is the main factor in the degradation of the SC efficiency characteristics over time. Therefore, this layer should have an optimal thickness (~1.2 nm) [12]. Consequently, it is necessary to remove a thick oxide layer and grow a new one of optimal thickness. Since the resulting PEDOT:PSS film is porous after solvent evaporation, especially after washing out its PSS components, the PEDOT/Si interface of the manufactured elements is easily accessible for chemical processing. As a result, the SiO_2 interlayer was completely removed by immersing the fabricated heterojunction structure in an HF solution. Then, an oxide film of controlled thickness was grown by thermal oxidation.

Table 3. Long-term stability of light *I–V* characteristic parameters of SCs heterostructures based on PEDOT:PSS/GaAs heterojunction with quasigrating interface.

	U_{oc}, mV	I_{sc}, mA/cm^2	f, %	R_s, Ohm	R_{sh}, Ohm	η, %
As-prepared	531	9.9	56.3	6.89	320.4	2.97
Next day	564	12.7	63.0	4.86	587.5	4.51
14 days	547	13.2	62.9	4.74	871.0	4.53
67 days	526	13.2	59.5	4.91	588.1	4.11

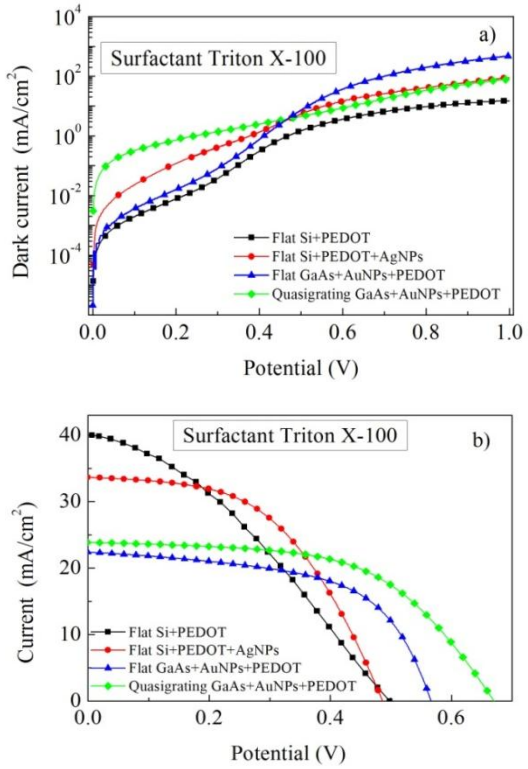

Fig. 6. Direct dark (*a*) and light (*b*) *I–V* characteristics of SC structures based on PEDOT:PSS/Si and PEDOT:PSS/GaAs heterojunctions.

The optimum is achieved by etching with 10% HF for 30 s followed by annealing at 150 °C for 15...30 s. At the same time, a tunnel-thin SiO_2 intermediate layer was formed and, as a result, the efficiency of planar structures was increased from 4.5% to 7.3%, mainly due to an increase in I_{sc} as shown in Fig. 5b.

Fig. 6 shows the *I–V* characteristics of SC structures with flat and quasigrating type GaAs interfaces with Au NPs. Compared with Si, both structures show larger U_{oc} values that are associated with large band bending, and smaller I_{sc} due to the larger GaAs band gap. In this case, a more positive effect of Au NPs was observed, presumably since gold forms a higher surface barrier with GaAs than with Si. The fill factor f is larger here, which is caused by Au NPs and low series resistance. In general, the efficiency (6.6%) approaches the best value for Si (7.3%), but these SCs have the greatest advantage in the long-term stability of parameters.

Moreover, in the case of GaAs, the characteristics remain fairly stable for 1-2 months, while for SC structures based on Si, the characteristics usually deteriorate rapidly over time (in just a few days, the efficiency decreases to 0). The presented in Table 3 results of measurements of light *I–V* characteristics (Fig. 7) show that the next day all characteristics of the GaAs-based structures improved significantly. Particularly, the efficiency increased 1.5 times due to the increase in U_{oc}, I_{sc}, fill factor f and shunt resistance R_{sh}, and reduction in the series resistance R_s. It can be explained by GaAs self-passivation and the growth of an oxide of optimal thickness under the PEDOT:PSS film on the relief surface when the PEDOT:PSS contacts the textured surface. After 14 days, the characteristics of GaAs-based heterojunction were changed slightly, and after 67 days, the efficiency was decreased by 9.2% relative to the previous measurement, which is caused by the decrease in U_{oc}, f, R_{sh}, and an increase in R_s, probably due to a too large increase in the thickness of the oxide on the heterojunction interface.

After all, it is known that the natural oxide film on gallium arsenide monocrystal surface grows much more slowly [34, 35] than on silicon [12]. Therefore, comparing the behavior of SC characteristics based on the organic film on different semiconductor substrates one can conclude that it is not the organic film that degrades, but the interface of heterojunction. Therefore, our results show that a separate study is required to search for methods to stabilize the heterojunction interface parameters, especially in the case of Si substrate.

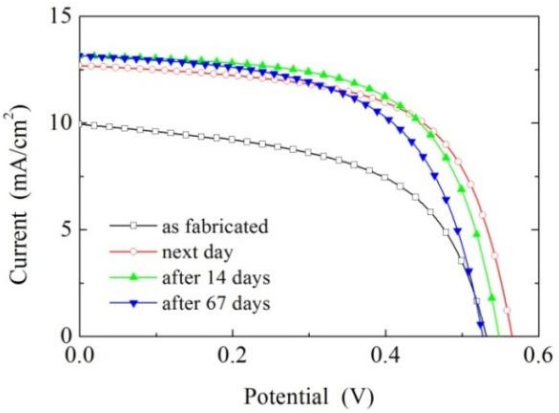

Fig. 7. Light *I–V* characteristics of SC structure based on PEDOT:PSS/GaAs heterojunction with quasigrating interface.

4. Conclusions

Few methods for increasing the efficiency of solar cells based on PEDOT:PSS/Si(GaAs) heterojunctions have been considered. It has been found that the texturing of the semiconductor surface, the deposition of plasmon active Ag or Au nanoparticles on the heterojunction interface increases the efficiency of photoconversion of heterostructures due to an increase in light absorption, a decrease in the structure series resistance, and increase the *I–V* characteristic fill factor of the corresponding SC structures.

It is shown that the multi-stage deposition of an organic film with intermediate washings with ethanol leads to an increase in its conductivity at smaller film thicknesses due to the removal of the non-conductive PSS component and the filling of the voids with PEDOT globules, which improves the current flow conditions.

A post-processing treatment method for fabricated SCs is proposed. It allows obtaining an intermediate SiO_2 layer of optimal thickness, which is a critical factor affecting the efficiency of PEDOT:PSS/Si structures.

Unlike heterostructures on Si, GaAs-based SC heterostructures demonstrate more stable characteristics over a long time and higher open-circuit voltages. Comparing the stability of heterojunction characteristics on different semiconductor substrates, one can ascertain that it is not the PEDOT:PSS film that degrades, but probably the thickness of the tunnel oxide at the interface of heterojunction is changed. Thus, organic thin-film heterostructures require additional efforts to seal the active interface of the heterojunction from air access.

Acknowledgments

This work was supported by the NATO SPS project G6197 “Plasmonically Enhanced Perovskite Thin-Film Solar Cells”. The authors express their gratitude to the National Academy of Sciences of Ukraine for support within the framework of the project 0125U000799 “New physical principles and technologies for the development of the element base of modern infrared photoelectronics”.

References

1. Gao P., Yang Z., He J. *et al.* Dopant-free and carrier-selective heterocontacts for silicon solar cells: recent advances and perspectives. *Adv. Sci*. 2017. **5**, No 3. P. 1700547. https://doi.org/10.1002/advs.201700547.
2. He J., Gao P., Ling Z. *et al.* High-efficiency silicon/organic heterojunction solar cells with improved junction quality and interface passivation. *ACS Nano*. 2016. **10**, No 12. P. 11525–11531. https://doi.org/10.1021/acsnano.6b07511.
3. Jäckle S., Liebhaber M., Gersmann C. *et al.* Potential of PEDOT:PSS as a hole selective front contact for silicon heterojunction solar cells. *Sci. Rept*. 2017. **7**, No 1. P. 2170. https://doi.org/10.1038/s41598-017-01946-3.
4. Liu Q., Ishikawa R., Funada S. *et al.* Highly efficient solution-processed poly(3,4-ethylenedioxythiophene):poly(styrenesulfonate)/crystalline-silicon heterojunction solar cells with improved light-induced stability. *Adv. Energy Mater.* 2015. **5**, No 17. P. 1500744. https://doi.org/10.1002/aenm.201500744.
5. Shahrim N.A., Ahmad Z., Azman A.W. *et al.* Mechanisms for doped PEDOT:PSS electrical conductivity improvement. *Mater. Adv.* 2021. **2**, No 22. P. 7118–7138. https://doi.org/10.1039/d1ma00290b.
6. Song I., Park N.Y., Jeong G.S., *et al.* Conductive channel formation for enhanced electrical conductivity of PEDOT:PSS with high work-function. *Appl. Surf. Sci.* 2020. **529**. P. 147176. https://doi.org/10.1016/j.apsusc.2020.147176.
7. Otieno F., Shumbula N.P., Airo M. *et al.* Improved efficiency of organic solar cells using Au NPs incorporated into PEDOT:PSS buffer layer. *AIP Advances*. 2017. **7**, No 8. P. 085302. https://doi.org/10.1063/1.4995803.
8. Fung D.D.S., Qiao L., Choy W.C.H. *et al.* Optical and electrical properties of efficiency enhanced polymer solar cells with Au nanoparticles in a PEDOT–PSS layer. *J. Mater. Chem*. 2011. **21**, No 41. P. 16349–16356. https://doi.org/10.1039/c1jm12820e.
9. Iwan A., Boharewicz B., Tazbir I. *et al.* Silver nanoparticles in PEDOT:PSS layer for polymer solar cell application. *Int. J. Photoenergy*. 2015. **2015**. P. 764938. https://doi.org/10.1155/2015/764938.
10. Singh P., Srivastava S.K., Sivaiah B. *et al.* Enhanced photovoltaic performance of PEDOT:PSS/Si solar cells using hierarchical light trapping scheme. *Solar Energy*. 2018. **170**. P. 221–233. https://doi.org/10.1016/j.solener.2018.05.048.
11. Li C., He Z., Wang Q. *et al.* Performance improvement of PEDOT:PSS/*n*-Si heterojunction solar cells by alkaline etching. *Silicon*. 2021. **14**, No 5. P. 2299–2307. https://doi.org/10.1007/s12633-021-01034-2.
12. Zhang C., Zhang Y., Guo H. *et al.* Efficient planar hybrid *n*-Si/PEDOT:PSS solar cells with power conversion efficiency up to 13.31% achieved by controlling the SiO_x interlayer. *Energies.* 2018. **11**, No 6. P. 1397. https://doi.org/10.3390/en11061397.
13. Li X. Metal assisted chemical etching for high aspect ratio nanostructures: A review of characteristics and applications in photovoltaics. *Curr. Opin. Solid State Mater. Sci*. 2012. **16**, No 2. P. 71–81. https://doi.org/10.1016/j.cossms.2011.11.002.
14. Mamykin S., Mamontova I., Kotova N. *et al.* Nanocomposite solar cells based on organic/inorganic (clonidine/Si) heterojunction with plasmonic Au nanoparticles. *Phys. Chem. Solid State.* 2020. **21**, No 3. P. 390–398. https://doi.org/10.15330/pcss.21.3.390-398.
15. Dmitruk N.L., Borkovskaya O.Y., Dmitruk I.N., Mamontova I.B. Analysis of thin film surface barrier solar cells with a microrelief interface. *Sol. Energy Mater. Sol. Cells*. 2003. **76**, No 4. P. 625–635. https://doi.org/10.1016/S0927-0248(02)00272-6.

16. Dmitruk N.L., Borkovskaya O.Yu., Mamykin S.V. *et al.* Au/GaAs photovoltaic structures with single-wall carbon nanotubes on the microrelief interface. *SPQEO*. 2015. **18**. P. 31–35. https://doi.org/10.15407/spqeo18.01.031.
17. Dmitruk N., Barlas T., Dmytruk A., Korovin A., Romanyuk V. Synthesis of 1D regular arrays of gold nanoparticles and modeling of their optical properties. *J. Nanosci. Nanotechnol*. 2008. **8**, No 2. P. 564–571. https://doi.org/10.1166/jnn.2008.a137.
18. Kondratenko S., Lysenko V., Gomeniuk Y. *et al.* Charge carrier transport, trapping, and recombination in PEDOT:PSS/*n*-Si solar cells. *ACS Appl. Energy Mater*. 2019. **2**, No 8. P. 5983–5991. https://doi.org/10.1021/acsaem.9b01083.
19. Jiang Y., Gong X., Qin R. *et al.* Efficiency enhancement mechanism for poly(3,4-ethylene-dioxythiophene):poly(styrenesulfonate)/silicon nanowires hybrid solar cells using alkali treatment. *Nanoscale Res. Lett*. 2016. **11**, No 1. P. 267. https://doi.org/10.1186/s11671-016-1450-5.
20. Mamykin S.V., Mamontova I.B., Lunko T.S. *et al.* Fabrication and conductivity of thin PEDOT:PSS-CNT composite films. *SPQEO*. 2021. **24**. P. 148–153. https://doi.org/10.15407/spqeo24.02.148.
21. Schroder D.K. *Semiconductor Material and Device Characterization*. 2nd ed. New York, USA: John Wiley & Sons, Inc. 1998.
22. Horii T., Hikawa H., Katsunuma M., Okuzaki H. Synthesis of highly conductive PEDOT:PSS and correlation with hierarchical structure. *Polymer*. 2018. **140**. P. 33–38. https://doi.org/10.1016/j.polymer.2018.02.034.
23. Li Q., Yang J., Chen S. *et al.* Highly conductive PEDOT:PSS transparent hole transporting layer with solvent treatment for high performance silicon/organic hybrid solar cells. *Nanoscale Res. Lett*. 2017. **12**, No 1. P. 506. https://doi.org/10.1186/s11671-017-2276-5.
24. Alemu D., Wei H.-Y., Ho K.-C., Chu C.-W. Highly conductive PEDOT:PSS electrode by simple film treatment with methanol for ITO-free polymer solar cells. *Energy Environ. Sci.* 2012. **5**. No 11. P. 9662–9671. https://doi.org/10.1039/c2ee22595f.
25. Ouyang J. Solution-processed PEDOT:PSS films with conductivities as indium tin oxide through a treatment with mild and weak organic acids. *ACS Appl. Mater. Interfaces*. 2013. **5**, No 24. P. 13082–13088. https://doi.org/10.1021/am404113n.
26. Yu Z., Xia Y., Du D., Ouyang J. PEDOT:PSS films with metallic conductivity through a treatment with common organic solutions of organic salts and their application as a transparent electrode of polymer solar cells. *ACS Appl. Mater. Interfaces*. 2016. **8**, No 18. P. 11629–11638. https://doi.org/10.1021/acsami.6b00317.
27. Xia Y., Ouyang J. Salt-induced charge screening and significant conductivity enhancement of conducting poly(3,4-ethylenedioxythiophene):poly (styrenesulfonate). *Macromolecules*. 2009. **42**, No 12. P. 4141–4147. https://doi.org/10.1021/ma900327d.
28. Fujiwara H. *Spectroscopic Ellipsometry: Principles and Applications*. Chichester, Great Britain: John Wiley & Sons, Ltd. 2007.
29. Kondratenko O.S., Mamykin S.V., Lunko T.S., *et al.* Optical characterization of hybrid PEDOT:PSS/Si heterostructures by spectroscopic ellipsometry. *Mol. Cryst. Liq. Cryst*. 2021. **717**, No 1. P. 92–97. https://doi.org/10.1080/15421406.2020.1860533.
30. Sze S.M. *Physics of Semiconductor Devices*. 2nd ed. New York, USA: John Wiley and Sons. 1981.
31. Qi B., Wang J. Fill factor in organic solar cells. *Phys. Chem. Chem. Phys*. 2013. **15**, No 23. P. 8972–8982. https://doi.org/10.1039/c3cp51383a.
32. Sheng J., Fan K., Wang D. *et al.* Improvement of the SiO_x passivation layer for high-efficiency Si/PEDOT:PSS heterojunction solar cells. *ACS Appl. Mater. Interfaces*. 2014. **6**, No 18. P. 16027–16034. https://doi.org/10.1021/am503949g.
33. Sun Z., He Y., Xiong B. *et al.* Performance-enhancing approaches for PEDOT:PSS-Si hybrid solar cells. *Angew. Chem. Int. Ed.* 2020. **60**, No 10. P. 5036–5055. https://doi.org/10.1002/anie.201910629.
34. Feng L., Zhang L., Liu H. *et al.* Characterization study of native oxides on GaAs(100) surface by XPS. *Proc. SPIE*8912, *International Symposium on Photoelectronic Detection and Imaging 2013: Low-Light-Level Technology and Applications*. 2013. P. 89120N. https://doi.org/10.1117/12.2033679.
35. Moriarty P., Hughes G. An investigation of the early stages of native oxide growth on chemically etched and sulfur-treated GaAs(100) and InP(100) surfaces by scanning tunnelling microscopy. *Ultramicroscopy*. 1992. **42-44**, Part 1. P. 956–961. https://doi.org/10.1016/0304-3991(92)90385-w.

Authors' contributions

Mamykin S.V.: conceptualization, resources, investigation, formal analysis, writing – original draft, writing – review & editing.
Lunko T.S.: sample preparation, investigation of electro-physical parameters.
Mamontova I.B.: sample preparation, investigation of electro-physical parameters, writing – original draft, visualization.
Kondratenko O.S.: optical parameters investigation, formal analysis.
Barlas T.R.: formal analysis, investigation.
Kotova N.V.: resources.
Semikina T.V.: formal analysis, investigation.
Dmitruk I.M.: investigation, writing – review & editing.
Berezovska N.I.: investigation, writing – review & editing.
Hrabovskyi Ye.S.: structural investigation.
Romanyuk V.R.: optical parameters investigation and analysis, visualization, writing – review & editing.

Authors and CV

S.V. Mamykin, PhD in Physics and Mathematics, Head of the Department of Kinetic phenomena and polaritonics at the V. Lashkaryov Institute of Semiconductor Physics, NASU. The area of his scientific interests includes optoelectronics, plasmonics, optics, nanophotonics, sensors and photodetectors.
https://orcid.org/0000-0002-9427-324X

T.S. Lunko, junior researcher at the Department of Kinetic phenomena and polaritonics, V. Lashkaryov Institute of Semiconductor Physics, NASU. The area of scientific interests includes heterojunction solar cells, including organic/inorganic ones.
E-mail: havrylenko@isp.kiev.ua,
https://orcid.org/0000-0001-9476-2409

I.B. Mamontova, PhD in Physics and Mathematics, researcher at the Department of Kinetic phenomena and polaritonics at the V. Lashkaryov Institute of Semiconductor Physics, NASU. The area of scientific interests includes development of technology and experimental study of the properties of heterojunction solar cells and barrier structures.
E-mail: mirina@isp.kiev.ua,
https://orcid.org/0000-0003-0368-3065

O.S. Kondratenko, PhD in Physics and Mathematics, senior researcher at the Department of Diagnostics of semiconductor materials, structures and devices, Laboratory of spectral ellipsometry, V. Lashkaryov Institute of Semiconductor Physics, NASU.
The area of scientific interests includes optoelectronics, plasmonics, optics, nanophotonics, thin films.
E-mail: kondratenko@isp.kiev.ua,
https://orcid.org/0000-0003-1948-4431

T.R. Barlas, PhD in Physics and Mathematics, Senior Researcher at the Department of Kinetic phenomena and polaritonics, V. Lashkaryov Institute of Semiconductor Physics, NASU. The area of scientific interests includes development of technology and research of nanocomposite materials based on porous semiconductors.
E-mail: barlas@isp.kiev.ua,
https://orcid.org/0000-0001-8483-9257

N.V. Kotova, junior researcher at the Department of Kinetic phenomena and polaritonics V. Lashkaryov Institute of Semiconductor Physics, NASU. The area of scientific interests includes development of technology for chemical and electrochemical methods for processing semiconductors and the creation of nanocomposite materials. E-mail: nvkotova@bizbooks.com.ua,
https://orcid.org/0000-0001-7787-795X

T.V. Semikina. PhD in Physics and Mathematics, senior researcher at the V. Lashkaryov Institute of Semiconductor Physics, NASU. The area of scientific interests includes technology of semiconductor films and structures for functional electronics and nanoelectronics, complex structural, electrical and optical studies of new materials.
E-mail: tanyasemikina@gmail.com,
https://orcid.org/0000-0002-6182-4703

I.M. Dmitruk is Doctor of Physical and Mathematical Sciences, Professor of the Department of Experimental Physics at the Taras Shevchenko National University of Kyiv. The area of scientific interests includes atom physics, electronic processes in nanostructures, optics, spectroscopy of crystals, modern physics problems, condensed matter photonics. E-mail: igor_dmytruk@knu.ua,
http://orcid.org/0000-0001-9482-8746

N.I. Berezovska is PhD in Physics and Mathematics, Senior Researcher of Faculty of Physics at the Taras Shevchenko National University of Kyiv. The area of scientific interests includes study of the morphology and energy structure of metal-semiconductor composites, porous materials, different LIPSS for photovoltaics and sensorics.
E-mail: nataliya.berezovska@knu.ua,
https://orcid.org/0000-0002-6967-6426

Ye.S. Hrabovskyi is engineer of the Department of Experimental Physics at the Taras Shevchenko National University of Kyiv. The area of scientific interests includes fabrication and investigations of the nanostructured and porous materials.
E-mail: hrabovskye@gmail.com,
https://orcid.org/0000-0003-4078-0569

V.R. Romanyuk, PhD in Physics and Mathematics, Senior Researcher of the Department of Kinetic phenomena and polaritonics at the V. Lashkaryov Institute of Semiconductor Physics, NAS of Ukraine. The area of scientific interests includes optical materials science and optical diagnostics.
E-mail: romanyuk@isp.kiev.ua,
https://orcid.org/0000-0002-0068-5973

Порівняння оптичних та фотовольтаїчних характеристик сонячних елементів на основі гетеропереходів органічних нанокомпозитних плівок на Si та GaAs

С.В. Мамикін, Т.С. Лунько, І.Б. Мамонтова, О.С. Кондратенко, Т.Р. Барлас, Н.В. Котова, Т.В. Сємікіна, І.М. Дмитрук, Н.І. Березовська, Є.С. Грабовський, В.Р. Романюк

Анотація. Проведено порівняння між гетероструктурами сонячних елементів на основі органічних композитних тонких плівок полі(3,4-етилендіокситіофен)-полі(стиролсульфонат) (PEDOT:PSS) і напівпровідників (Si, GaAs) з плоскою та мікрорельєфною межею поділу. Товщини плівок PEDOT:PSS та оптичні параметри було отримано за допомогою спектральної еліпсометрії, тоді як електрична провідність для постійного струму була визначена за допомогою чотиризондового методу. Запропоновано спосіб підвищення електропровідності плівок PEDOT:PSS шляхом формування багатошарової плівки зі зниженим вмістом PSS компоненти. Наночастинки плазмон-активного металу (Au, Ag) було вирощено на активній межі поділу для підвищення ефективності фотоперетворення. Вони зменшують послідовний опір структури і збільшують коефіцієнт заповнення ВАХ та поглинання падаючого світла. Запропоновано метод пост-обробки виготовлених структур, який дозволяє отримати тунельно-тонкий проміжний шар SiO_2 оптимальної товщини. Фотоелектричні властивості виготовлених сонячних елементів показали, що структури на основі GaAs мають більш стабільні довгострокові характеристики та вищу напругу розімкненого кола, ніж структури на основі Si.

Ключові слова: гетероперехід, сонячні елементи, мікрорельєф, PEDOT:PSS, металеві наночастинки, пост-обробка.